THE ASTROPHYSICAL JOURNAL, 223:56–73, 1978 July 1

SPECTROPHOTOMETRY OF SEYFERT 2 GALAXIES AND NARROW-LINE RADIO GALAXIES*

ALAN T. KOSKI
Lick Observatory, Board of Studies in Astronomy and Astrophysics, University of California, Santa Cruz
Received 1977 September 16; accepted 1978 January 11

ABSTRACT

Spectrophotometric scans of 20 Seyfert 2 galaxies, three intermediate Seyfert galaxies, and five narrow-line radio galaxies are presented. The emission-line spectra are similar in all the galaxies. A wide range of levels of ionization is present. The average density in the line-emitting gas is about 2000 cm^{-3}, and the average temperature is about 12,000–25,000 K. The strengths of lines of neutral atoms and singly ionized ions are correlated with each other, while the strengths of lines of higher-ionization ions are separately correlated with each other. Two galaxies were observed to have velocity differences between lines from the low and high ionization regions. The velocity differences are less than the emission-line widths which are typically 500–600 km s^{-1}.

The continua of all the galaxies show stellar absorption features and an ultraviolet excess when compared with galaxies with no emission lines. The continua of these galaxies can be represented well by a normal-galaxy continuum which is diluted by an underlying power-law continuum. If the assumed power-law continuum extends to high frequency, then there are enough ultraviolet photons to photoionize H and He and thus to account for the observed strengths of the recombination lines.

Comparison of emission-line strengths in these galaxies with that in planetary nebulae and the Crab Nebula suggests that the source of ionization is probably ultraviolet radiation. Photoionization models by MacAlpine show general agreement with these emission-line spectra.

Subject headings: galaxies: internal motions — galaxies: Seyfert — radio sources: general — spectrophotometry

I. INTRODUCTION

A spectrophotometric survey of radio galaxies which were known to have emission lines in their optical spectrum has been carried out at Lick Observatory. Osterbrock, Koski, and Phillips (1975) and Osterbrock (1976) have found that the spectra of radio galaxies separate into two classes: about one-fourth have broad permitted emission lines with widths many thousands of km s^{-1}, while three-fourths have narrow emission lines of about 500 km s^{-1} width. These two classes are very similar to the two classes of Seyfert galaxies (Weedman and Khachikian 1969; Khachikian and Weedman 1971, 1974). The survey at Lick Observatory was extended to the Seyfert galaxies to compare their spectra with those of radio galaxies. Comparison of the two classes of Seyfert galaxies suggested an intermediate class (Osterbrock and Koski 1976): present in the spectrum is a broad Balmer-line component (characteristic of a Seyfert 1 spectrum) and a narrow Balmer-line component with a strong forbidden-line spectrum (characteristic of a Seyfert 2 spectrum), such as in NGC 4151.

The present study considers the optical spectra of the narrow-line radio galaxies and of the Seyfert 2 galaxies. Points of interest are the relationship between these two types of objects, how they compare, how they differ. We want to know if the Seyfert 2 galaxies form a homogeneous class, or if they separate into subclasses. Exactly how are the Seyfert 2 galaxies related to the intermediate class? Finally, we will determine some of the physical conditions in the emitting gas in these galaxies.

The five radio galaxies reported here were chosen from Schmidt (1965), Burbidge and Strittmatter (1972), and Burbidge (1970). The Seyfert galaxies were selected from the list of Khachikian and Weedman (1974). Those which appeared to be Seyfert 2 galaxies are included here (Koski 1976). Also included are NGC 6764, which was noted to be a Seyfert 2 galaxy by Rubin, Thonnard, and Ford (1975), and Mrk 573, similarly noted by J. Huchra at the Minkowski Symposium, 1976 Berkeley A.S.P. meeting. Sargent (1970) questions whether I Zw 81 has broad emission lines in its spectrum, and thus might be a Seyfert galaxy. (Note that Sargent refers to this galaxy as I Zw 80, but according to Zwicky [1971] it is I Zw 81.) Markarian and Lipovetsky note that Mrk 378 is a very compact object (1971) and predict Seyfert characteristics for Mrk 700 (1974). Included in the discussions which follow are observations of the narrow-line radio galaxy Cygnus A by Osterbrock and Miller (1975) and of five others by Costero and Osterbrock (1977) and of the intermediate Seyfert galaxy NGC 4151 by Osterbrock and Koski (1976).

II. OBSERVATIONS

The observations presented here were obtained with the image-dissector-scanner (Robinson and Wampler

* *Lick Observatory Bulletin*, No. 786.

1972, 1973) attached to the new spectrograph (Miller, Robinson, and Wampler 1976) at the Cassegrain focus of the 3 m Shane telescope at Lick Observatory. Observations made of 3C 33 and 3C 184.1 before 1974 January were made with the old spectrograph mentioned in the earlier references.

A projected slit size of 2".7 × 4".0 and a grating with 600 grooves mm^{-1} gave 2400 Å coverage with 10 Å resolution (full width at half-maximum of comparison emission lines). Each object except I Zw 81 was observed from at least shorter than λ3727 to longward of λ6731 in the rest system of the galaxy. Two overlapping scans, a blue one and a red one, were obtained to accomplish this.

Observations with the new spectrograph were obtained between 1974 September and 1976 July. Typical integration times were about 32 minutes in each of the blue and red regions for objects brighter than magnitude 15 and 64 to 96 minutes each for fainter objects. Dates and specific integration times are given by Koski (1976).

The routine reduction to absolute energy units and a linear wavelength scale is detailed by Osterbrock and Miller (1975), Costero and Osterbrock (1977), and Koski (1976). Representative scans are shown in Figure 1 and are composites of the blue and red scans.

III. EMISSION-LINE SPECTRUM

The emission-line spectra of the galaxies presented here are very rich. The Balmer lines of H I are present in all these galaxies with a decrement steeper than that resulting from pure recombination. Except for three cases, the only other permitted lines observed are those of He I and He II. Fe II permitted lines are observed in Mrk 42, 5C 3.100, and weakly in NGC 1068. In fact, the spectra of Mrk 42 and 5C 3.100 are more characteristic of Seyfert 1 galaxies (though the emission lines in both these objects are narrow enough to put them in the Seyfert 2 or narrow-line radio-galaxy group): relatively weak forbidden lines (compared to the Balmer lines) and relatively strong blends of Fe II permitted lines in the regions around λλ4570, 5190, and 5320. Forbidden lines arise from a wide range of ionization: [N (I, II)], [O (I, II, III)], [Ne (III, V)], [S (II, III)], [Ar (III, IV, V)], [Ca V], and [Fe (III, VII, X)].

a) Emission-Line Intensities

The emission lines in these galaxies are superposed on a continuous spectrum with absorption lines characteristic of galaxies containing stars. Two general types of continua are present: those with H I absorption lines and those without them. Since the lower members of the Balmer series (Hα, Hβ, Hγ) are generally in emission, the presence or absence of H I absorption lines is determined by the presence or absence of the higher members in absorption, usually H9 and H10, λλ3835, 3798. The absorption lines due to stars in these galaxies mask the weak emission lines and hence must be removed. The absorption-line removal is accomplished by subtracting the continuum of a galaxy which has no emission lines.

The average spectrum of the elliptical galaxies NGC 6482 and NGC 6702 was used to remove the absorption-line continuum of the emission-line galaxies with no H I absorption lines, while the earlier-type spectrum of the Sa galaxy NGC 2681 was used for those with H I absorption. Details of the subtraction process are given by Koski (1976), and examples are shown by Koski and Osterbrock (1976) and Costero and Osterbrock (1977). Those galaxies with Balmer absorption lines are Mrk 198, Mrk 268, Mrk 507, and Mrk 700. In addition, NGC 6764 and I Zw 81 have weak H I absorption lines; for these two galaxies both galaxy continua were used in the subtraction process, and the results were averaged. The Balmer absorption lines in Mrk 700 are much stronger than in NGC 2681. Equivalent-width comparisons with two early spectral type standard stars, Feige 15 and Feige 56, were used to correct the emission-line strengths in this galaxy. The subtraction of the absorption lines generally left an emission-line spectrum on a very smooth, nearly featureless continuum which was nonzero.

The emission-line intensities were measured by summing the intensity in each channel in the line above an interpolated continuum. The total intensities of line blends were measured in this manner. A deblend program was used to separate the blended lines: [Ne III] λ3869 + He I λ3889, Hγ + [O III] λ4363, [O III] λ4959 + λ5007, [N II] λ6548 + λ6583 + Hα, and [S II] λ6716 + λ6731. A single line, usually [O III] λ5007 (or Hβ when stronger), was used to synthesize the observed spectrum. The line spacing was determined by the laboratory wavelengths of the lines and the galaxy redshift. Individual line intensities and widths could be varied to improve the fit. As each parameter was varied, the trial spectrum was subtracted from the observed spectrum. The best parameter fit was that which yielded the flattest subtraction.

The observed line intensities with respect to Hβ, $F/F(\mathrm{H}\beta)$, are given in Table 1. The order is by decreasing strength of $I([\mathrm{O\ III}]\lambda5007)/I(\mathrm{H}\beta)$. Note that [Fe VII] λ6087 is blended with [Ca V] λ6087 which has a strength $I([\mathrm{Ca\ V}]\lambda6087) = I([\mathrm{Ca\ V}]\lambda5309)/5.1$ (Garstang 1968). The observed flux $F(\mathrm{H}\beta)$ is also given. The reddening-corrected intensities $I/I(\mathrm{H}\beta)$ (see § II*b* below) for the objects in Table 1 are given in Table 2.

The narrow components of the emission lines of the intermediate Seyfert galaxies were measured in the manner described above. In addition, the narrow component of Hα and nearby forbidden lines were subtracted from the Hα complex to leave only the broad component of Hα. This was then used as a profile to remove the broad components of the other Balmer lines and He I and He II lines. The broadening was scaled by the wavelength to give the best subtraction. The observed fluxes $F/F(\mathrm{H}\beta n)$ and reddening-corrected intensities $I/I(\mathrm{H}\beta n)$ with respect to the narrow component of Hβ for the intermediate Seyfert galaxies are given in Table 3.

The line strengths for the two galaxies with strong Fe II emission, Mrk 42 and 5C 3.100, are given in Table 4. The Fe II multiplets are given in parentheses. Among the stronger Fe II emission lines in NGC 1068

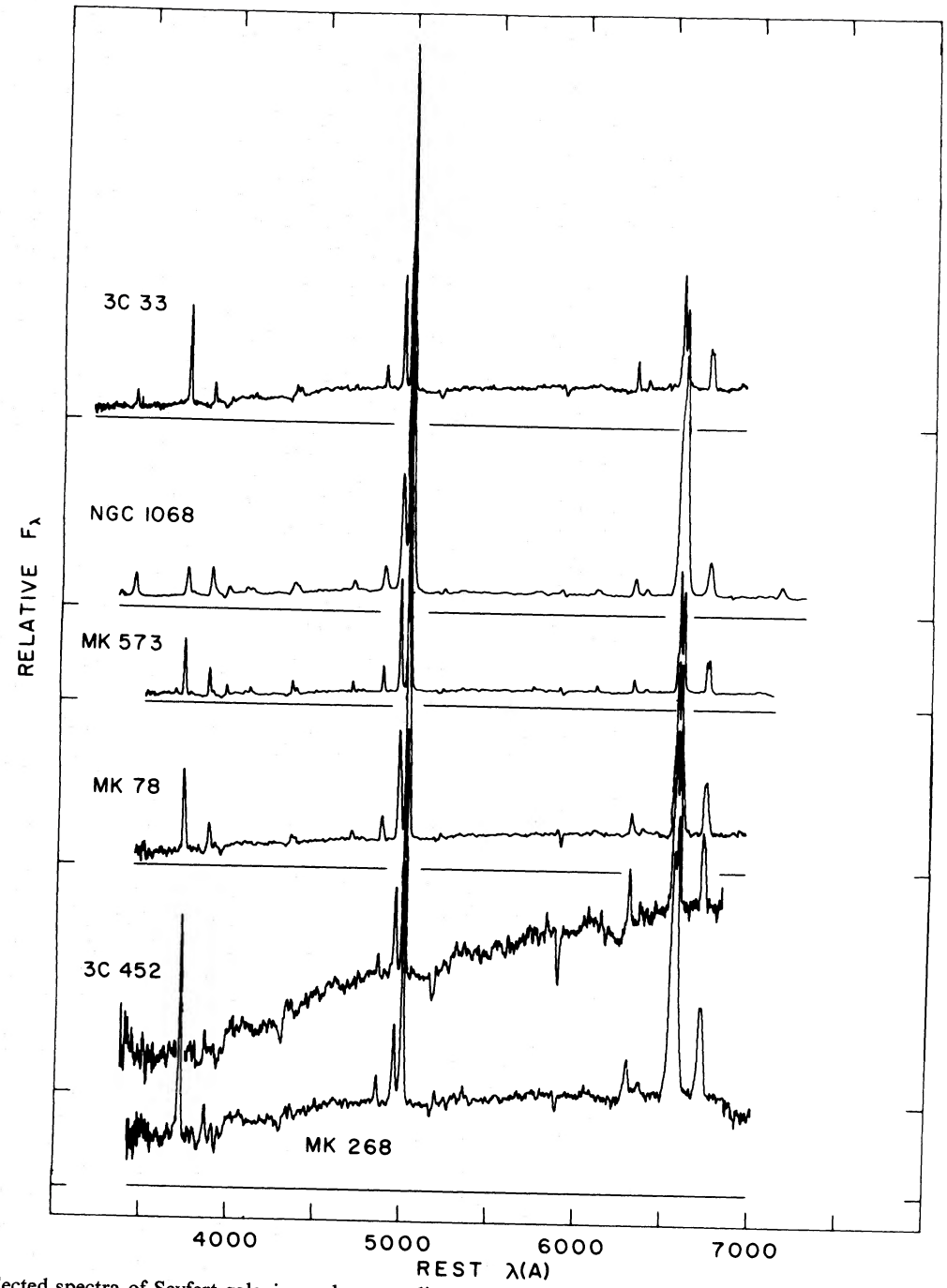

FIG. 1.—Selected spectra of Seyfert galaxies and narrow-line radio galaxies in relative energy units per unit wavelength versus wavelength in the rest system of the galaxy. Order is by decreasing strength of $I(\lambda 5007)/I(\mathrm{H}\beta)$ corrected for reddening. At the end are two intermediate Seyfert galaxies and Mrk 42 with strong Fe II emission in its spectrum.

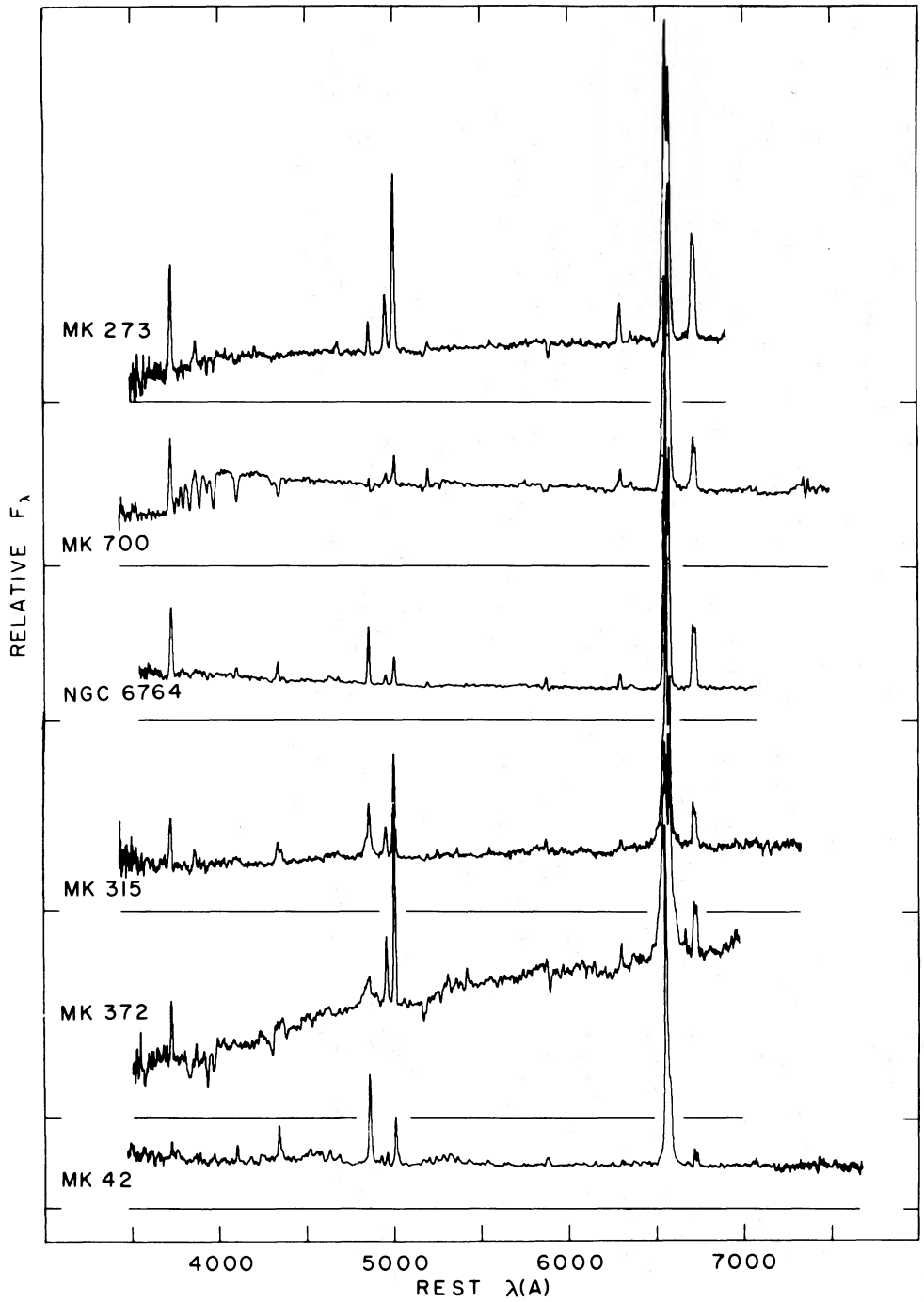

FIG. 1.—*Continued*

are those with estimated observed fluxes with respect to Hβ: multiplets (37, 38) λλ4515, 4521 ≤ 0.05, (48, 49) λ5317 ≤ 0.05, (48) λ5363 ≤ 0.03, and (49) λ5425 ≤ 0.03.

The accuracy of the line intensity measurements depends upon the photon statistics, the flux calibration from standard stars, the correction for underlying absorption lines, and the placement of the interpolated continuum. The relative intensities $F/F(\mathrm{H}\beta)$ of strong unblended lines agree between scans taken on different nights to about 10%. The accuracy of weaker lines and blended profiles is about ±20%. Very weak lines with accuracy about a factor of 2 are noted in the tables by a colon.

Comparison of the measures of NGC 1068 reported here with photographic measures by Osterbrock and Parker (1965), photographic and photoelectric measures by Anderson (1970), and photoelectric measures by Wampler (1971) and by Shields and Oke (1975) shows agreement of the observed fluxes to about 15% for lines and blends with strength greater than or equal to $F(\mathrm{H}\beta)$. The relative strength of Hα and [N II] λλ6548 + 6583 differs by factors of 2–3, however. Since the total strength of the blend agrees well, the discrepancy is probably due to different techniques for de-blending the complex.

The strength of the broad component of Hα and Hβ of Mrk 372 varied from 1975 October to 1975 December, an interval of 77 days. The data for Mrk 372 are consistent with the continuum flux, the flux in the forbidden lines, and the flux in the narrow components of Hα and Hβ having remained constant. The scan in Figure 1 and the line intensities in Table 3 are averages of the data from the two dates. Although the strengths increased by about 60%, the decrement remained nearly constant, ~7.1, and the line profiles retained the same width and shape. Other broad components, which are weaker than Hβ were not observed to change.

b) *Reddening*

Figure 2 is a plot of the Balmer decrement Hα, Hβ, Hγ. Various types of galaxies are represented by various symbols. Note that there is no segregation of any of the types. There is reasonable agreement between the observed Balmer decrement and the reddening trajectory, considering the uncertainties of the corrections for absorption lines and blends. Assuming the Balmer decrement is due to recombinations, the reddening of the Balmer lines may be found from Figure 2.

The reddening of the forbidden lines may be assumed to be the same as for the Balmer lines. However, Angel *et al.* (1976) showed that the permitted and forbidden lines in NGC 1068 are polarized by different amounts and at different position angles. They suggest that the permitted-line emitting region is different from the forbidden-line emitting region. The reddening of the lines may also be different. Wampler (1971, also 1968) and Shields and Oke (1975) measured the strengths of the [S II] blue λ4071 and infrared λ10320 lines which permit the reddening of the [S II] lines to be found (Miller 1968). Shields and Oke found a reddening which corresponds to $E_{B-V} = 0.4$, while Wampler found $E_{B-V} = 0.5$. The Balmer decrement reported here implies $E_{B-V} = 0.52 \pm 0.05$, consistent with the [S II] line reddening. This suggests that in spite of the difference in polarization properties, the reddening of the permitted lines gives a good estimate of the reddening of the forbidden lines.

The effect of reddening may be written

$$\log I(\lambda) = cf(\lambda) + \log F(\lambda) + \text{constant}, \quad (1)$$

where c is the measure of the amount of reddening, and $f(\lambda)$ is the reddening curve. A least-squares fit was made of equation (1) to the recombination decrement and the observed Balmer decrement for each galaxy. Equal weights were used, which corresponds to equal percentage errors in the observed line intensities. The Whitford reddening curve as parametrized by Miller and Mathews (1972) and the case B Balmer recombination decrement given by Brocklehurst (1971): $I(\mathrm{H}\alpha:\mathrm{H}\beta:\mathrm{H}\gamma:\mathrm{H}\delta) = 2.85:1.00:0.469:0.259$ for $T = 10^4$ K and $N_e = 10^4$ cm^{-3} were used. Generally, three Balmer lines, Hα, Hβ, and Hγ, were used to determine the reddening. In about half the cases, uncertain values of Hδ were not used. The reddening c ($= E_{B-V}/0.72$) with a typical uncertainty ±0.1 is given in Tables 2, 3, and 4 along with the reddening-corrected intensities.

c) *Densities and Temperatures*

The average density and temperature in the line-emitting gas in these galaxies may be found from reddening-corrected forbidden-line strengths. Equations for the temperature-sensitive line ratios of [O I], [N II], and [O III] are found in Seaton (1975) and Osterbrock (1974). The density-sensitive lines [O II] λλ3726, 3729 could not be resolved in these galaxies, both because of the velocity widths of the lines and because of the 10 Å resolution of the scans. The equation for the density-sensitive line ratio of [S II] λλ6716, 6731 was derived from a three-level-atom calculation. Five-level-atom calculations by Balick (1975, private communication) give the line ratios of [O II] λλ3727, 7319, 7330 and of [S II] λλ4071, 6716, 6731 which are sensitive to both temperature and density.

A range of densities and temperatures is undoubtedly present in these galaxies, judging from the wide range of ionizations. An order-of-magnitude estimate of the density and temperature is that point in the density-temperature plane which most closely reproduces the observed line ratios. These values are listed in Table 5 along with values determined the same way for Cygnus A (Osterbrock and Miller 1975) and the five narrow-line radio galaxies reported by Costero and Osterbrock (1977). Uncertain values are indicated by colons, and the low-density limit is indicated LDL. The range of average temperatures is about 4.0 to 4.4 in the log (10,000–25,000 K), and the average log N_e = 3.3 (2000 cm^{-3}).

TABLE 1

OBSERVED RELATIVE EMISSION-LINE INTENSITIES IN SEYFERT 2 GALAXIES AND NARROW-LINE RADIO GALAXIES

Line		Mrk 176	3C 33	Mrk 3	NGC 1068	Mrk 573	Mrk 78	Mrk 348	Mrk 34	Mrk 1	3C 184.1	3C 433
3346	[Ne V]		...		0.19					0.14	0.29	
3426	[Ne V]		0.54		0.72					0.49	0.68	
3727	[O II]	1.70	3.47	2.21	0.76	2.11	2.55	3.05	2.61	1.61	1.69	3.62
3760	[Fe VII]	...	...	0.038	0.10	0.093	0.068:	...	0.051	0.059	...	...
3869	[Ne III]	1.53	1.02	0.94	0.94	1.01	1.07	1.23	0.87	1.08	0.76	1.21
3889	He I + H	...	0.14	0.18	0.12	0.17	...	0.19	0.14	0.14	0.33	0.19:
3967	[Ne III] + H	0.23:	0.34	0.41	0.37	0.32	0.24	0.37	0.34	0.38	0.34	0.34:
4071	[S II]	0.48	0.17	0.26	0.21	0.15	0.14	0.28	0.15	0.43	0.039:	0.24:
4102	Hδ	...	0.18	0.21	0.16	0.26	0.12	0.15:	0.23	0.17	0.23	0.38:
4340	Hγ	0.090:	0.38	0.39	0.34	0.41	0.27	0.37	0.42	0.32	0.39	0.43
4363	[O III]	0.22	0.27	0.19	0.17	0.15	0.098	0.21	0.13	0.16	0.29	0.31:
4471	He I	...	...	0.029	0.046	0.039	...	0.049	0.046	0.041:	0.045:	...
4658	[Fe III]	...	0.080	0.028	0.067	0.052	0.070	0.066	0.043	0.067	...	...
4686	He II	0.38	0.24	0.17	0.38	0.34	0.31	0.20	0.27	0.27	0.26	...
4711	[Ar IV]	0.21	0.10	0.034	0.045	0.074	0.052	0.078	0.068	0.048	...	...
4740	[Ar IV]	0.20	0.062	0.040	0.059	0.064	0.042	0.043	0.057	0.059	...	...
4861	Hβ	1.00	1.00	1.00	1.00	1.00	1.00	1.00	1.00	1.00	1.00	1.00
4959	[O III]	5.00	4.22	4.16	4.28	4.01	4.11	3.96	3.76	3.73	3.32	3.53
5007	[O III]	15.79	13.27	13.46	13.22	12.64	13.02	12.33	11.87	11.75	11.08	10.11
5159	[Fe VII]	0.28	0.10:	0.042	0.034	0.050	0.072	0.089	0.026	0.034	...	...
5199	[N I]	0.094	0.13	0.15	0.11	0.081	0.14	0.14	0.085	0.060	...	0.31
5309	[Ca V]	0.31	0.092:	0.019	0.056:	0.052	0.030:	0.047:	0.044	0.031:	...	...
5412	He II	0.055	...	0.019	0.037:	...	...	...	0.032	...	...	...
5528	[Cl III]	0.11	...	0.031	0.027:	...	0.075:	0.061	...	...	...	...
5577	[O I]	0.048	...	0.014	0.017:	...	0.092:	0.058	0.019	...	...	...
5721	[Fe VII]	0.25:	0.073	0.026	0.061:	0.11	...	...	0.043	0.039:	...	...
5755	[N II]	...	0.060	0.066	0.029:	...	0.050	0.091:	0.040	0.032:	...	...
5876	He I	0.18	0.13	0.12	0.21	0.13	0.17	0.16	0.14	0.16	0.17	0.46
6087	[Fe VII] + *	0.33	0.14	0.097	0.22	0.18	0.13	0.17	0.078	0.14	...	...
6300	[O I]	0.85	0.98	1.14	0.62	0.43	0.62	1.58	0.45	1.19	0.29	1.17
6312	[S III]	...	...	0.11:	...	0.081	...	...	...	...	...	...
6364	[O I]	0.30	0.33	0.38	0.24	0.12	0.21	0.52	0.14	0.47	0.12	0.33
6374	[Fe X]	0.29	...	0.13:	0.047	0.060	...	...	...	...	0.051:	...
6435	[Ar V]	0.17	0.051	0.023:	0.057	...	0.056:	...	0.034	...	0.072:	...
6548	[N II]	2.31	0.90	1.72	2.70	1.19	1.57	1.14	0.96	1.44	0.31	3.85
6563	Hα	6.55	3.95	5.31	4.47	4.30	5.31	4.27	4.10	5.00	3.88	6.26
6583	[N II]	7.02	2.66	5.48	7.94	3.62	5.04	3.54	3.00	4.17	0.87	9.54
6601	[Fe VII]	0.77	...	0.15:	0.24	0.058:	0.50:	...	0.036	...	...	...
6678	He I	...	...	0.040:	0.096	0.067	0.14	...	0.052	...	0.12	...
6716	[S II]	1.37	1.34	1.30	0.48	1.12	1.55	1.74	1.14	0.96	0.38	3.04
6731	[S II]	1.35	1.13	1.46	0.99	1.21	1.40	2.01	1.12	1.02	0.45	2.19
7006	[Ar V]	...		0.025	0.050:	...		...		...		
7065	He I	0.28:		0.042	0.059			0.13		...		
7136	[Ar III]	0.64		0.34	0.51			0.44		0.80:		
7325	[O II]	0.31:										
F(Hβ) †		6.7(-15)	4.4(-15)	2.1(-13)	1.6(-12)	5.2(-14)	2.2(-14)	2.8(-14)	3.9(-14)	3.0(-14)	4.9(-15)	1.1(-15)

TABLE 1 (continued)

Line		Mrk 270	III Zw 55	3C 452	Mrk 198	Mrk 268	Mrk 273	I Zw 81	Mrk 298	Mrk 507	Mrk 700	NGC 6764	Mrk 378
3346	[Ne V]												
3426	[Ne V]												
3727	[O II]	4.81	1.33	2.86	2.01	2.69	3.05		3.10	0.46	1.11	1.35	...
3760	[Fe VII]	...	...	...	0.10	...	...		...	...	...	...	...
3869	[Ne III]	1.22	0.69	0.86	0.46	0.61	0.71		0.18	0.16	0.20	0.050:	...
3889	He I + H	0.13:	...	0.17	0.22	0.093	...		0.083	0.089:	...	0.068	...
3967	[Ne III] + H	0.46	...	0.28	0.27	0.36	0.19		0.073	0.073:	0.11:	0.017:	...
4071	[S II]	0.29	0.26:	0.15:	0.12	0.28	0.076:		0.13	...	...	0.087:	...
4102	Hδ	0.31:	...	0.11:	0.28	0.38:	0.16:		0.14:	...	...	0.19	...
4340	Hγ	0.49	...	0.38	0.45	0.52	0.25:		0.35	0.24	...	0.32	...
4363	[O III]	0.26	0.16:	0.14	0.11	0.21:	0.13:		0.039:	0.048:	...	0.031:	...
4471	He I	...	...	...	...	...	...		...	...	...	0.021:	...
4658	[Fe III]	...	...	...	0.047	0.074	...	...	...	...	...	0.014	...
4686	He II	0.21	0.17	0.054	0.072	0.074	0.28	...	...	...	...	0.057	...
4711	[Ar IV]	0.036	...	...	0.041:	0.038	...	0.15:	...	...	...	0.022:	...
4740	[Ar IV]	0.043	...	...	0.041:	0.051	...	0.10:	...	...	...	...	...
4861	Hβ	1.00	1.00	1.00	1.00	1.00	1.00	1.00	1.00	1.00	1.00	1.00	1.00
4959	[O III]	3.00	2.55	2.51	1.82	1.60	1.66	0.98	0.66	0.23	0.18	0.15	...
5007	[O III]	8.89	7.75	7.32	5.72	5.03	5.06	3.14	2.03	0.81	0.55:	0.53	0.49
5159	[Fe VII]	0.090	...	0.072	0.041	0.074	0.058	0.16:	0.031:	...	...	0.020:	...
5199	[N I]	0.12	0.26	0.22	0.15	0.30	0.22	0.46	0.089	...	0.30	0.083	...
5309	[Ca V]	0.067	...	0.099	...	0.14:	...	...	...	...	...	0.019:	...
5412	He II	...	0.10	0.16	0.035	...	...	...	...	...	...	...	...
5528	[Cl III]	...	...	...	0.045	0.13:	...	...	...	...	...	...	...
5577	[O I]	0.054	0.13:	...	...	...	...	...	...	...	...	0.032:	...
5721	[Fe VII]	...	...	...	0.048	...	...	...	...	...	...	0.026:	...
5755	[N II]	...	0.066:	...	...	...	...	...	...	...	...	0.024:	0.48:
5876	He I	0.21	0.18:	0.25	0.13	0.12	0.096	0.47	0.14	0.12:	0.040:	0.17	0.32
6087	[Fe VII] + *	0.054:	...	0.14	...	0.10	...	...	...	...	...	0.019:	...
6300	[O I]	0.95	1.36	1.93	0.46	1.08	1.22	0.46	0.58	0.17	0.38	0.26	0.18:
6312	[S III]	...	...	...	...	...	...	...	...	...	...	...	...
6364	[O I]	0.28	0.45	0.65	0.13	0.36	0.29	...	0.19	...	0.13	0.080	...
6374	[Fe X]	...	...	...	...	...	...	...	...	...	...	0.040:	...
6435	[Ar V]	...	...	...	...	...	...	...	0.041	...	...	...	...
6548	[N II]	1.14	2.97	2.50	0.89	2.15	2.80	1.60	0.34	1.34	1.91	1.33	0.93
6563	Hα	3.78	7.88	5.43	3.89	4.96	9.32	6.93	4.12	5.48	3.36	5.66	5.95
6583	[N II]	3.53	10.78	6.56	2.92	7.27	8.38	4.68	1.08	3.56	5.89	3.85	2.86
6601	[Fe VII]	...	...	...	...	...	...	...	...	...	...	...	...
6678	He I	0.15	...	0.26	0.046	...	...	0.20:	0.092	...	...	0.041	...
6716	[S II]	1.47	1.94	2.09	1.17	1.93	3.05	1.43	1.02	0.47	0.71	1.06	1.12
6731	[S II]	1.70	2.20	1.46	0.90	1.63	1.87	0.88	0.82	0.46	0.70	1.00	0.84
7006	[Ar V]	...	...		...						...	...	
7065	He I	...	...								...	0.036:	
7136	[Ar III]		0.59:								...		
7325	[O II]		...										
F(Hβ)†		2.3(-14)	4.5(-15)	1.1(-15)	1.8(-14)	1.5(-14)	6.0(-15)	3.7(-15)	1.9(-14)	7.3(-15)	2.3(-14)	5.4(-14)	1.7(-15)

* blended with [Ca V] λ6087.

† erg cm^{-2} s^{-1}

TABLE 2

REDDENING-CORRECTED RELATIVE EMISSION-LINE INTENSITIES IN SEYFERT 2 GALAXIES AND NARROW-LINE RADIO GALAXIES

Line		Mrk 176	3C 33	Mrk 3	NGC 1068	Mrk 573	Mrk 78	Mrk 348	Mrk 34	Mrk 1	3C 184.1	3C 433
3346	[Ne V]		...		0.36					0.30	0.41	
3426	[Ne V]		0.86		1.34					1.00	0.96	
3727	[O II]	3.54	4.93	3.52	1.23	2.92	4.96	4.45	3.43	2.78	2.21	6.17
3760	[Fe VII]	...	...	0.060	0.16	0.13	0.13:	...	0.066	0.099	...	...
3869	[Ne III]	2.91	1.39	1.42	1.43	1.35	1.92	1.71	1.10	1.73	0.96	1.92
3889	He I + H	...	0.19	0.27	0.17	0.23	...	0.27	0.18	0.22	0.41	0.30:
3967	[Ne III] + H	0.40:	0.46	0.59	0.55	0.42	0.42	0.51	0.43	0.59	0.42	0.52:
4071	[S II]	0.81	0.22	0.37	0.30	0.19	0.22	0.36	0.18	0.63	0.047:	0.34:
4102	Hδ	...	0.23	0.28	0.23	0.33	0.18	0.20:	0.28	0.24	0.27	0.54:
4340	Hγ	0.13:	0.46	0.50	0.44	0.49	0.38	0.45	0.49	0.43	0.44	0.57
4363	[O III]	0.32	0.32	0.24	0.22	0.18	0.14	0.26	0.15	0.21	0.33	0.41:
4471	He I	...	...	0.035	0.056	0.044	...	0.057	0.051	0.050:	0.050:	...
4658	[Fe III]	...	0.086	0.030	0.074	0.055	0.080	0.071	0.045	0.075	...	...
4686	He II	0.43	0.26	0.18	0.41	0.36	0.35	0.22	0.28	0.30	0.27	...
4711	[Ar IV]	0.23	0.11	0.036	0.049	0.077	0.057	0.082	0.071	0.052	...	...
4740	[Ar IV]	0.22	0.065	0.043	0.062	0.066	0.045	0.045	0.059	0.063	...	...
4861	Hβ	1.00	1.00	1.00	1.00	1.00	1.00	1.00	1.00	1.00	1.00	1.00
4959	[O III]	4.69	4.10	3.99	4.11	3.89	3.88	3.83	3.68	3.56	3.25	3.37
5007	[O III]	14.36	12.68	12.67	12.42	12.12	11.94	11.74	11.46	10.95	10.70	9.44
5159	[Fe VII]	0.23	0.094:	0.037	0.030	0.046	0.061	0.081	0.024	0.029	...	...
5199	[N I]	0.076	0.12	0.13	0.097	0.074	0.12	0.12	0.079	0.051	...	0.27
5309	[Ca V]	0.24	0.080:	0.016	0.047:	0.046	0.023:	0.041:	0.040	0.025:	...	...
5412	He II	0.040	...	0.015	0.030:	...	...	...	0.028	...	...	...
5528	[Cl III]	0.072	...	0.025	0.021:	...	0.053:	0.049	...	...	...	...
5577	[O I]	0.032	...	0.011	0.013:	...	0.063:	0.046	0.016	...	...	...
5721	[Fe VII]	0.15:	0.058	0.019	0.044:	0.089	...	...	0.036	0.027:	...	...
5755	[N II]	...	0.047	0.048	0.021:	...	0.032	0.070:	0.033	0.022:	...	...
5876	He I	0.10	0.096	0.084	0.15	0.10	0.10	0.12	0.12	0.10	0.14	0.31
6087	[Fe VII] + *	0.17	0.099	0.064	0.14	0.14	0.072	0.12	0.061	0.086	...	...
6300	[O I]	0.40	0.68	0.71	0.38	0.31	0.31	1.07	0.34	0.68	0.22	0.68
6312	[S III]	...	...	0.069:	...	0.058	...	...	...	...	...	...
6364	[O I]	0.14	0.23	0.23	0.14	0.085	0.10	0.35	0.11	0.26	0.088	0.19
6374	[Fe X]	0.13	...	0.080:	0.028	0.042	...	...	...	...	0.039:	...
6435	[Ar V]	0.076	0.034	0.014:	0.034	...	0.027:	...	0.025	...	0.054:	...
6548	[N II]	1.00	0.60	1.01	1.56	0.82	0.73	0.74	0.70	0.77	0.23	2.09
6563	Hα	2.81	2.63	3.10	2.57	2.95	2.46	2.76	2.99	2.66	2.85	3.38
6583	[N II]	2.99	1.76	3.18	4.55	2.47	2.32	2.28	2.18	2.21	0.64	5.13
6601	[Fe VII]	0.33	...	0.087:	0.14	0.040:	0.23:	...	0.026	...	...	...
6678	He I	...	...	0.023:	0.054	0.045	0.063	...	0.037	...	0.084	...
6716	[S II]	0.56	0.87	0.73	0.26	0.75	0.68	1.09	0.82	0.49	0.27	1.58
6731	[S II]	0.54	0.73	0.82	0.55	0.80	0.61	1.25	0.80	0.52	0.32	1.13
7006	[Ar V]	...		0.013	0.026:	...		...		...		
7065	He I	0.10:		0.022	0.031			0.077		...		
7136	[Ar III]	0.23		0.18	0.26			0.25		0.37:		
7325	[O II]	0.10:										
c		1.1	0.53	0.70	0.72	0.49	1.0	0.57	0.41	0.82	0.40	0.8

TABLE 2 (continued)

Line		Mrk 270	III Zw 55	3C 452	Mrk 198	Mrk 268	Mrk 273	I Zw 81	Mrk 298	Mrk 507	Mrk 700	NGC 6764	Mrk 378
3346	[Ne V]												
3426	[Ne V]												
3727	[O II]	5.64	3.19	4.81	2.51	3.75	8.27		4.49	1.02	1.27	2.43	...
3760	[Fe VII]	...	...	...	0.12	...	...		...	...	...	...	...
3869	[Ne III]	1.40	1.50	1.36	0.56	0.82	1.70		0.25	0.33	0.22	0.084:	...
3889	He I + H	0.14:	...	0.27	0.27	0.12	...		0.12	0.18:	...	0.11	...
3967	[Ne III] + H	0.52	...	0.42	0.32	0.47	0.41		0.098	0.14:	0.12:	0.027:	...
4071	[S II]	0.32	0.50:	0.22:	0.14	0.36	0.16:		0.17	...	...	0.13:	...
4102	Hδ	0.35:	...	0.16:	0.33	0.47:	0.31:		0.17:	...	...	0.28	...
4340	Hγ	0.53	...	0.50	0.50	0.61	0.42:		0.43	0.37	...	0.43	...
4363	[O III]	0.28	0.25:	0.18	0.12	0.25:	0.22:		0.047:	0.072:	...	0.042:	...
4471	He I	...	...	...	...	...	...		...	...	...	0.026:	...
4658	[Fe III]	...	...	...	0.049	0.079	...	...	...	...	...	0.015	...
4686	He II	0.22	0.20	0.059	0.075	0.078	0.33	...	...	...	...	0.062	...
4711	[Ar IV]	0.037	...	...	0.043:	0.039	...	0.16:	...	...	...	0.024:	...
4740	[Ar IV]	0.044	...	...	0.042:	0.052	...	0.11:	...	...	...	...	...
4861	Hβ	1.00	1.00	1.00	1.00	1.00	1.00	1.00	1.00	1.00	1.00	1.00	1.00
4959	[O III]	2.96	2.36	2.40	1.79	1.55	1.52	0.91	0.64	0.21	0.18	0.14	...
5007	[O III]	8.71	6.92	6.85	5.56	4.82	4.44	2.84	1.94	0.73	0.54:	0.49	0.45
5159	[Fe VII]	0.086	...	0.063	0.039	0.068	0.045	0.14:	0.028:	...	...	0.017:	...
5199	[N I]	0.11	0.20	0.19	0.14	0.28	0.16	0.37	0.080	...	0.29	0.070	...
5309	[Ca V]	0.063	...	0.082	...	0.12:	...	...	...	...	...	0.015:	...
5412	He II	...	0.068	0.13	0.031	...	...	...	...	...	...	...	...
5528	[Cl III]	...	...	...	0.040	0.11:	...	...	...	...	...	...	...
5577	[O I]	0.049	0.076:	...	...	...	...	...	...	...	...	0.023:	...
5721	[Fe VII]	...	...	...	0.041	...	...	...	...	...	...	0.018:	...
5755	[N II]	...	0.036:	...	...	...	...	...	...	...	...	0.016:	0.30:
5876	He I	0.19	0.090:	0.17	0.11	0.095	0.045	0.26	0.10	0.064:	0.036:	0.11	0.19
6087	[Fe VII] + *	0.047:	...	0.091	...	0.075	...	...	...	...	...	0.012:	...
6300	[O I]	0.81	0.56	1.14	0.37	0.77	0.44	0.21	0.40	0.077	0.33	0.14	0.089:
6312	[S III]	...	...	...	...	...	...	...	...	...	...	...	...
6364	[O I]	0.23	0.18	0.38	0.10	0.25	0.10	...	0.13	...	0.11	0.043	...
6374	[Fe X]	...	...	...	...	...	...	...	...	...	...	0.022:	...
6435	[Ar V]	...	...	...	...	...	...	...	0.028	...	...	...	...
6548	[N II]	0.95	1.08	1.38	0.69	1.47	0.89	0.66	0.22	0.54	1.64	0.68	0.43
6563	Hα	3.14	2.86	2.98	3.02	3.38	2.94	2.86	2.68	2.18	2.88	2.88	2.76
6583	[N II]	2.93	3.87	3.58	2.26	4.94	2.62	1.92	0.70	1.40	5.04	1.95	1.32
6601	[Fe VII]	...	...	...	...	...	...	...	...	...	...	...	...
6678	He I	0.12	...	0.14	0.035	...	...	0.079:	0.058	...	...	0.020	...
6716	[S II]	1.21	0.66	1.10	0.89	1.28	0.89	0.56	0.65	0.18	0.60	0.52	0.49
6731	[S II]	1.39	0.74	0.77	0.68	1.08	0.54	0.34	0.52	0.17	0.59	0.49	0.37
7006	[Ar V]	...	...		...						...	...	
7065	He I	...	...								...	0.016:	
7136	[Ar III]		0.17:								...		
7325	[O II]		...										
c		0.24	1.32	0.78	0.33	0.5	1.5	1.15	0.56	1.2	0.2	0.88	1.0

* blended with [Ca V] λ6087.

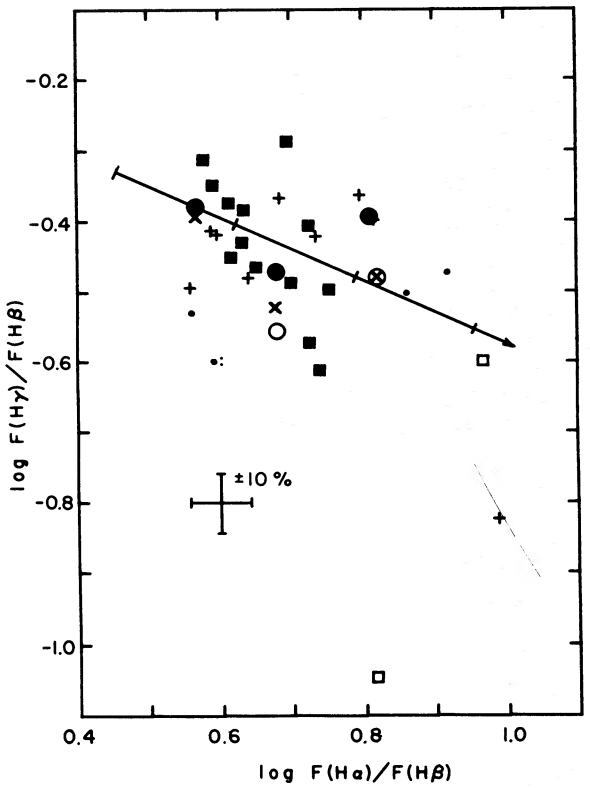

FIG. 2.—Observed Hα/Hβ/Hγ ratios for Seyfert 2 galaxies (*squares*), radio galaxies including those from Costero and Osterbrock (1977) (*pluses*), Cygnus A from Osterbrock and Miller (1975) (circled ×), intermediate Seyfert galaxies including NGC 4151 from Osterbrock and Koski (1976) (*large circles*, narrow components; *dots*, broad components), and galaxies with strong Fe II emission (×). Uncertain values are indicated by an open symbol or colon (:). The reddening trajectory extends from case B recombination decrement and is marked at reddening values $c = 0.5, 1.0, 1.5$.

d) Emission-Line Strength Correlations

Although somewhat similar average physical conditions exist in most of these galaxies, the strengths of the emission-line spectra are greatly different. The emission-line strengths were compared to search for any correlations which might distinguish the radio galaxies from the Seyfert galaxies.

The He I recombination line λ5876 shows no correlation with any other line. The relative strength of He I λ5876 is plotted against that of He II λ4686 in Figure 3. A wide range of He II is present, but there is only a relatively narrow range of He I. There are evidently various sizes of He^{++} zones but a more or less constant size of He^{+} zone compared to the H^{+} zone. For an assumed temperature $T = 16{,}000$ K and density $N_e = 2000\ cm^{-3}$, the average intensity

$$I(\text{He I } \lambda 5876)/I(\text{H}\beta) = 0.11$$

corresponds to a number density $N(He^{+})/N(H^{+}) = 0.09$, while $N(He^{++})/N(H^{+})$ ranges from 0 to 0.04. As a group, the Seyfert 2 galaxies and narrow-line radio galaxies have approximately normal He abundance.

Also shown in Figure 3 are correlations between lines from high-ionization ions He II, [Ne III], and [Ar III], and the λ5007 line of [O III]. Additional correlations of He II λ4686, and hence [O III] λ5007, were found (Koski 1976) with [Ne V] λ3426 (only a few measurements were available) and [Fe VII] λ6087. The [Fe VII] line was quite weak, and the correlation is rather poor.

The strengths of the lines of low-ionization ions are separately correlated with [S II] lines (Fig. 3). The correlations with the N lines is poorer because [N I] λ5199 is weak and blended with the Mg I *b* absorption feature, while [N II] λ6583 is blended with Hα. These lines are not correlated with the lines of high-ionization ions.

These line correlations suggest that there are two independent ionization zones in these galaxies: one of high ionization which includes He^{++}, O^{++}, Ne^{++}, Ne^{+4}, Ar^{++}, and probably Fe^{+6}, and one of low ionization which includes N^{0}, N^{+}, O^{0}, O^{+}, and S^{+}. This is further evidence for different physical conditions in different emitting regions as suggested by Osterbrock and Parker (1965), Anderson (1970), and others. Notice that there is no difference between the Seyfert galaxies and the radio galaxies plotted in Figure 3. The narrow components of the intermediate Seyfert galaxies appear to be the same as Seyfert 2 galaxies and narrow-line radio galaxies.

e) Emission-Line Widths

All the Seyfert and narrow-line radio galaxy emission-line profiles are broader than the profiles of comparison lines, which represent the instrumental profile to a good approximation. Galaxy emission-line profiles were compared with comparison lines which lay in the same part of the scan and which had been convolved with Gaussian profiles of various widths. The full widths at half-maximum intensity of the emission lines (forbidden and permitted, the narrow component for the intermediate Seyfert galaxies) are given in Table 6. The uncertainties refer to the approximate range of velocities found from different lines and from single lines using different comparison lines. Most of the velocities are less than the projected instrumental resolution of $600\ km\ s^{-1}$ (for 10 Å FWHM at 5000 Å) and thus result from rather subtle differences from the instrumental profile. Higher resolution scans of Mrk 573 obtained at the McGraw-Hill Observatory using the University of Michigan photon-counting multichannel spectrometer (Shectman and Hiltner 1976) yield an emission-line width of $340 \pm 40\ km\ s^{-1}$ (Feldman 1977), in excellent agreement with the value given here of $350 \pm 150\ km\ s^{-1}$.

The distribution of emission-line widths is shown in Figure 4. Various bin widths were used, depending upon the uncertainty of the value. The lines of Seyfert 2 galaxies and narrow-line radio galaxies and the narrow components of the intermediate Seyfert galaxies have the same distribution of widths. A

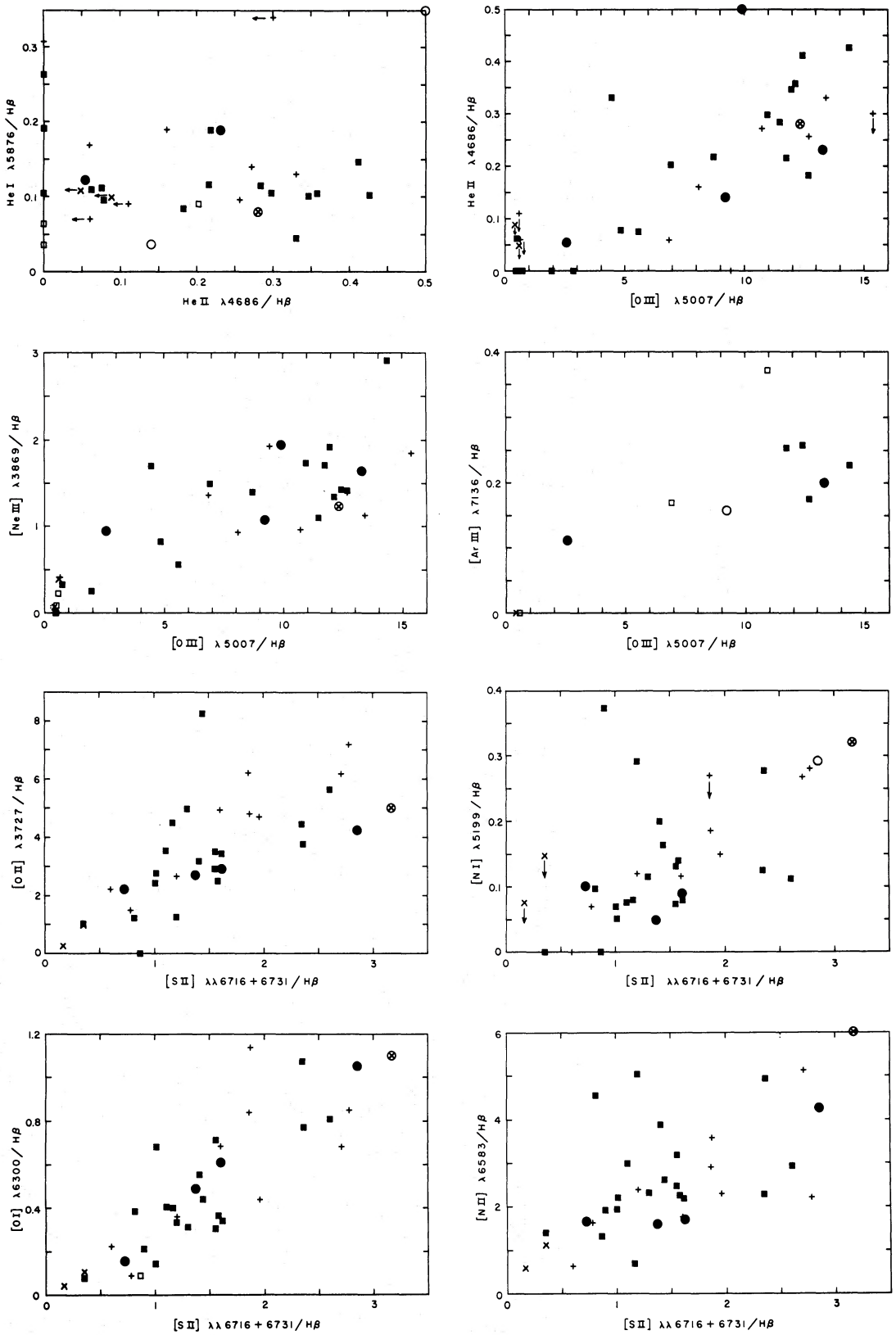

FIG. 3.—Correlations between line intensities. Reddening-corrected line intensities with respect to Hβ are plotted. The symbols are the same as in Fig. 2. He I line strength is not correlated with He II. High ionization lines are correlated with each other and with [O III] λ5007, while low ionization lines are separately correlated with each other and with [S II] λλ6716 + 6731.

TABLE 3

RELATIVE EMISSION-LINE INTENSITIES IN INTERMEDIATE-TYPE SEYFERT GALAXIES

Line		Mrk 6		Mrk 315		Mrk 372	
		F/F(Hβn)	I/I(Hβn)	F/F(Hβn)	I/I(Hβn)	F/F(Hβn)	I/I(Hβn)
3727	[O II]	1.70	2.71	1.22	2.21	2.66	4.23
3869	[Ne III]	0.71	1.07	0.56	0.94	1.30	1.95
3889	He I + H	0.13	0.19	...	...	...	...
3967	[Ne III] + H	0.31	0.45	0.20	0.32	...	...
4071	[S II]	0.17	0.24	0.10	0.16	...	...
4102	Hδn	0.19	0.26	0.051	0.078	...	...
4102	Hδb	...	...	0.37:	0.57:	...	...
4102	HδΣ	0.19	0.26	0.42:	0.65:	...	...
4340	Hγn	0.34	0.43	0.40	0.55	0.28:	0.35:
4340	Hγb	0.84	1.07	0.36:	0.50:	1.83	2.34
4340	HγΣ	1.18	1.50	0.76:	1.05:	2.11:	2.69:
4363	[O III]	0.15	0.19	0.18:	0.24:	0.28:	0.35:
4471	He I	0.047	0.057	...	...	...	...
4686	He II n	0.13	0.14	0.049	0.054	0.47	0.51
4686	He II b	...	...	0.64	0.71	...	...
4686	He II Σ	0.13	0.14	0.69	0.76	0.47	0.51
4861	Hβn	1.00	1.00	1.00	1.00	1.00	1.00
4861	Hβb	2.49	2.49	1.43	1.43	5.78	5.78
4861	HβΣ	3.49	3.49	2.43	2.43	6.78	6.78
4959	[O III]	3.13	3.00	0.92	0.87	3.39	3.25
5007	[O III]	9.78	9.21	2.76	2.56	10.53	9.92
5159	[Fe VII]	0.029:	0.026:	...	...	...	...
5199	[N I]	0.056	0.049	0.12	0.10	0.33:	0.29:
5412	He II	0.033	0.027	...	...	...	...
5721	[Fe VII]	0.031:	0.023:	...	...	...	...
5876	He I n	0.051:	0.036:	0.19	0.12	1.94:	1.36:
5876	He I b	0.62:	0.43:	0.92	0.58	2.06	1.44
5876	He I Σ	0.67:	0.47:	1.11	0.70	4.00:	2.80:
6087	[Fe VII] + *	0.093	0.061	...	...	...	...
6300	[O I]	0.78	0.49	0.28	0.16	1.69	1.05
6364	[O I]	0.28	0.17	0.099:	0.053:	0.66	0.40
6548	[N II]	0.95	0.56	1.11	0.56	2.08	1.22
6563	Hαn	4.76	2.78	6.47	3.24	4.79	2.80
6563	Hαb	20.72	12.10	5.60	2.80	41.39	24.16
6563	HαΣ	25.48	14.88	12.07	6.04	46.18	26.96
6583	[N II]	2.74	1.59	3.33	1.66	7.34	4.26
6716	[S II]	1.36	0.76	0.78	0.37	2.44	1.38
6731	[S II]	1.08	0.61	0.74	0.35	2.63	1.48
7065	He I	...	...	0.35:	0.15:		
7136	[Ar III]	0.30:	0.16:	0.26	0.11		
7325	[O II]	0.21:	0.10:				
F(Hβn)†		5.1(-13)		3.0(-14)		1.2(-14)	
c‡		1.3		0.8		1.18	

* blended with [Ca V] λ6087.

† erg cm^{-2} s^{-1}

‡ computed from narrow components of Balmer lines.

typical or average line width is about 500 to 600 km s^{-1}, comparable with the resolution of the scans presented here. Note that NGC 1068, often considered the prototype of Seyfert 2 galaxies, has a width of 1200 km s^{-1} and is the exception rather than the rule. The dip in the distribution between 500 and 600 km s^{-1} probably has no physical significance.

All the emission-line profiles of a galaxy had approximately the same shape and width. Nearly all the profiles appeared symmetrical and without structure. Mrk 700 had profiles which were asymmetric, with the blue side stronger in intensity. The profiles of Mrk 78 had a shoulder on the red side: possibly they are composed of two components each about 600 km s^{-1} wide and separated by about 600 km s^{-1}, with the redward component about one-third the strength of the other. Adams (1973) has previously reported in detail on the composite nature of the emission lines of Mrk 78.

f) *Redshift Differences*

Two redshift systems were found in Mrk 268 and in 5C 3.100. The [O III] λλ4959, 5007 lines had a different redshift from other lines with strengths greater than or equal to $F(H\beta)$. Phillips (1976) found a difference in redshifts in I Zw 1, a Seyfert 1 galaxy with strong Fe II emission. Phillips's results indicated two separate ionization regions: one of high ionization which included O^{++} and Ne^{++}, the other of low ionization

TABLE 4

RELATIVE EMISSION-LINE INTENSITIES IN GALAXIES WITH STRONG Fe II EMISSION

Line		Mrk 42		5C 3.100	
		F/F(Hβ)	I/I(Hβ)	F/F(Hβ)	I/I(Hβ)
3727	[O II]	0.19	0.26	0.55	0.97
3760	[Fe VII] + Fe II (29)	0.11	0.15	0.051:	0.088:
3783	Fe II (14)	0.028	0.037	0.045:	0.077:
3825	Fe II (29)	0.010:	0.013:	0.067	0.11
3869	[Ne III]	0.050:	0.065:	0.24	0.39
3889	He I + H	0.077	0.099	0.063	0.10
4002	Fe II (29)	0.015:	0.019:	...	...
4071	[S II]	0.046:	0.056:	0.15	0.22
4102	Hδ	0.18	0.23	0.087:	0.13:
4123	Fe II (28)	0.022:	0.027:	...	...
4129	Fe II (27)	0.012:	0.015:	...	...
4173	Fe II (27)	0.037	0.045	...	...
4179	Fe II (27)	0.058	0.070	0.069	0.098
4233	Fe II (27)	0.091	0.11	0.063:	0.089:
4258	Fe II (28)	0.076:	0.090:	0.022:	0.030:
4273	Fe II (27)	0.036	0.043	...	...
4297	Fe II (28)	0.036:	0.042:	0.047:	0.064:
4303	Fe II (27)	0.030:	0.035:	...	...
4340	Hγ	0.40	0.47	0.30	0.40
4352	Fe II (27)	0.025:	0.030:	0.018:	0.024:
4363	[O III]	0.055	0.064	0.060	0.080
4369	Fe II (28)	...	...	...	...
4385	Fe II (27)	0.050:	0.057:	0.11	0.15
4417	Fe II (27)	0.053	0.061	0.045:	0.058:
4473	Fe II (37)	0.067	0.075	0.047	0.059
4490	Fe II (37)	0.076	0.085	0.036:	0.045:
4508	Fe II (38)	0.069	0.076	0.076	0.093
4515	Fe II (37)	0.077	0.085	0.045	0.055
4521	Fe II (37,38)	0.081	0.089	0.11	0.14
4534	Fe II (37)	0.025:	0.028:	...	...
4542	Fe II (38)	0.047	0.052	0.060:	0.071:
4549	Fe II (38)	0.038:	0.041:	0.045	0.054
4556	Fe II (37)	0.10	0.11	0.063	0.075
4576	Fe II (38)	0.066	0.072	0.087:	0.10:
4583	Fe II (37,38)	0.082	0.088	0.12	0.14
4596	Fe II (38)	...	...	0.069	0.080
4621	Fe II (38)	0.047	0.051	0.024:	0.027:
4629	Fe II (37)	0.13	0.14	0.22	0.26
4648	Fe II (38)	0.021:	0.022:	0.018:	0.020:
4657	Fe II (43)	...	...	0.036:	0.040:
4667	Fe II (37)	0.054	0.057	0.089	0.099
4686	He II + Fe II (50)	0.084	0.088	0.043:	0.048:
4731	Fe II (43)	0.015	0.015	...	...
4861	Hβ	1.00	1.00	1.00	1.00
4924	Fe II (42)	0.095	0.093	0.072	0.070
4959	[O III]	0.13	0.13	0.19	0.18
5007	[O III]	0.43	0.41	0.63	0.58
5018	Fe II (42)	0.092	0.088	0.067	0.062
5159	[Fe VII]	0.031:	0.028:	0.051	0.044
5169	Fe II (42)	0.054	0.050	0.076	0.065
5198	[N I] + Fe II (49)	0.082	0.075	0.17	0.15
5235	Fe II (49)	0.081	0.073	0.065:	0.054:
5239	Fe II (41)	0.019:	0.017:	0.018:	0.015:
5257	Fe II (41)	0.047	0.043	0.047	0.039
5265	Fe II (48)	0.013:	0.012:	...	...
5276	Fe II (49)	0.076:	0.069:	0.047:	0.039:
5284	Fe II (41)	0.076:	0.068:	0.065:	0.053:
5309	[Ca V]	0.054	0.049	0.016:	0.013:
5317	Fe II (48,49)	0.063:	0.057:	0.12	0.096
5326	Fe II (49)	0.063:	0.056:	0.011:	0.009:
5338	Fe II (48)	0.042	0.038	...	...
5363	Fe II (48)	0.078	0.069	0.047:	0.037:
5425	Fe II (49)	0.048	0.042	...	...
5535	Fe II (55)	0.046	0.039	0.098	0.072
5631	[Fe VI]	0.024:	0.020:	...	...
5876	He I	0.12	0.099	0.17	0.11
5991	Fe II (46)	0.013:	0.010:	0.040:	0.025:
6087	Fe II (46)*	0.022:	0.017:	...	...
6148	Fe II (74)	0.052	0.040	0.056:	0.033:
6238	Fe II (74)	...	...	...	...
6248	Fe II (74)	0.038	0.029	...	...
6300	[O I]	0.056	0.042	0.19	0.11
6364	[O I]	0.021:	0.016:	...	...
6369	Fe II (40)	0.022:	0.016:	...	...
6374	[Fe X]	0.032:	0.023:	...	...
6417	Fe II (74)	0.054	0.039	...	...
6433	Fe II (40)	0.035:	0.025:	...	...
6456	Fe II (74)	0.040	0.029	...	...
6516	Fe II (40)	0.051	0.037	...	...
6548	[N II]	0.28	0.20	0.60	0.32
6563	Hα	3.69	2.63	4.75	2.47
6583	[N II]	0.83	0.59	2.17	1.12
6678	He I	0.040:	0.028:	0.047:	0.024:
6716	[S II]	0.12:	0.081:	0.45	0.23
6731	[S II]	0.12:	0.080:	0.25	0.12
7006	[Ar V]	0.022:	0.014:		
7065	He I	0.065:	0.044:		
F(Hβ)†		2.8(-14)		5.5(-15)	
c		0.44		0.85	

* blended with [Fe VII] and [Ca V] λ6087.

† erg cm^{-2} s^{-1}

TABLE 5

AVERAGE DENSITIES AND TEMPERATURES
IN SEYFERT 2 GALAXIES AND NARROW-LINE RADIO GALAXIES

Object	log T(°K)	log $N_e(cm^{-3})$	Object	log T(°K)	log $N_e(cm^{-3})$
Mrk 176	4.3	3.6:	I Zw 81	...	LDL
3C 33	4.1	2.9	Mrk 298	4.2	2.8
Mrk 3	4.1	3.5	Mrk 507	4.7:	3.5:
NGC 1068	4.0	4.2	Mrk 700	...	3.2:
Mrk 573	4.1	3.3	NGC 6764	4.2:	3.2
Mrk 78	4.0	3.2	Mrk 378	...	2.6:
Mrk 348	4.2	3.3	Mrk 6	4.2	2.9
Mrk 34	4.1	3.2	Mrk 315	4.4	3.3
Mrk 1	4.1	3.7:	Mrk 372	4.3:	3.4
3C 184.1	4.1	3.5	Mrk 42	4.8:	3.7:
3C 433	4.2	2.4	5C 3.100	4.7:	LDL
Mrk 270	4.2	3.4	Cyg A	4.0	3.0
III Zw 55	4.1	3.5	3C 98	4.3	3.6
3C 452	4.2	2.1	3C 178	...	3.2:
Mrk 198	4.1	2.6	3C 192	4.3	LDL
Mrk 268	4.3	3.0	3C 327	4.3	3.2
Mrk 273	4.3	LDL	PKS 2322-12	4.5:	2.1

LDL = low-density limit.

with H^+, Fe^+, Ca^+, N^+, and S^+. The redshifts of the [Ne III] λ3869 lines in Mrk 268 and 5C 3.100 are consistent with the [O III] redshifts. Table 7 lists these redshifts and the velocity differences between the redshift systems. Additional redshift differences have been found by Grandi (1977) and Feldman (1977). All the redshift differences are smaller than the emission-line widths. In five cases the high-ionization region has the lower redshift, but in Mrk 268 the reverse is true.

IV. CONTINUUM SPECTRUM

The continua present in the scans in Figure 1 result from the light from the background galaxy passing through the 2".7 × 4".0 slit and from any continuous spectrum in the nucleus. In contrast to the emission-line spectrum, the continuum ranges from insignificant

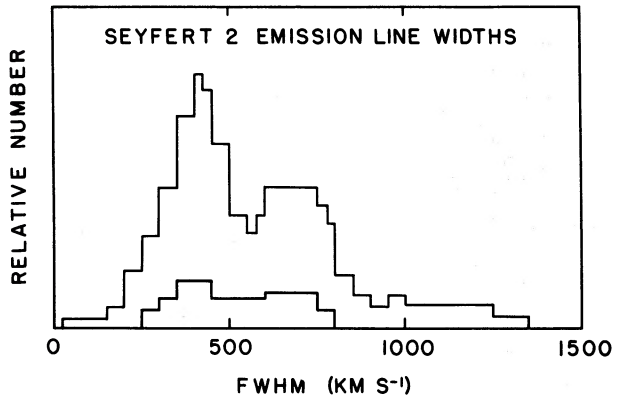

FIG. 4.—Distribution of emission-line widths. The full width at half-maximum intensity is shown for Seyfert 2 galaxies, narrow components of intermediate Seyferts, and narrow-line radio galaxies (*upper curve*) and for the narrow-line radio galaxies alone (*lower curve*). The half bin-width used in this graph was equal to the uncertainty of the measurement.

TABLE 6

EMISSION-LINE WIDTHS
IN SEYFERT 2 GALAXIES AND NARROW-LINE RADIO GALAXIES

Object	FWHM (km s^{-1})	Object	FWHM (km s^{-1})
Mrk 176	750 ± 150	Mrk 198	350 ± 150
3C 33	450 ± 100	Mrk 268	750 ± 100
Mrk 3	900 ± 150	Mrk 273	700 ± 100
NGC 1068	1200 ± 150	I Zw 81	225 ± 200
Mrk 573	350 ± 150	Mrk 298	350 ± 100
Mrk 78	1100 ± 150	Mrk 507	800 ± 200
Mrk 348	400 ± 50	Mrk 700	350 ± 150
Mrk 34	450 ± 100	NGC 6764	400 ± 100
Mrk 1	600 ± 150	Mrk 378	300 ± 150
3C 184.1	350 ± 100	Mrk 6	700 ± 100
3C 433	700 ± 100	Mrk 315	500 ± 100
Mrk 270	500 ± 100	Mrk 372	400 ± 100
III Zw 55	670 ± 100	Mrk 42	550 ± 100
3C 452	650 ± 100	5C 3.100	450 ± 150

in Mrk 3 and Mrk 348 to dominant in I Zw 81 and Mrk 378. It further ranges from very red as in 3C 452 to very blue as in Mrk 700 and NGC 6764.

With the exception of three galaxies (NGC 6764, Mrk 42, and 5C 3.100) all the continua appear to be chiefly due to an integrated stellar absorption-line spectrum. The three exceptions have very flat spectra which extend far into the blue. All the continua (including these three) have absorption lines of various strengths: G-band, Mg I *b*, a broad feature at approximately λ6230 due to TiO and many blended lines of Fe I and Ca I, as well as Na I D and Ca II K lines due in part perhaps to interstellar matter in the galaxies. The strengths of these lines suggest there is a component of the continuum which is continuous and which dilutes the integrated stellar absorption spectrum.

The strength of the component due to stars was found by subtracting a suitable galaxy spectrum with no emission lines. As noted in § III*a*, two kinds of absorption-line continua are present: those with Balmer lines in absorption, and those without. The absorption-line continuum was subtracted to leave a smooth, featureless continuum under the emission-line spectrum. The fraction of the continuum at λ4861 which was removed (and hence is due to stars) by this

TABLE 7

EMISSION-LINE REDSHIFT DIFFERENCES

Object	Redshift		ΔVel (km s^{-1})	FWHM (km s^{-1})	Source
	Ionization Low	Ionization High			
I Zw 1	0.0608	0.0587	600	1200	1
Mrk 268	0.0404	0.0410	-175	750	2
5C 3.100	0.0728	0.0718	280	450	2
PKS 1345+12	0.1214	0.1206	215	1400	3
NGC 7469	0.0163	0.0158	150	370	4
Mrk 618	0.0356	0.0344	350	600	4

Sources: (1) Phillips (1976); (2) Koski (1976); (3) Grandi (1977); (4) Feldman (1977).

TABLE 8

FIT OF POWER LAW AND REDDENING OF GALAXY CONTINUUM TO OBSERVED F_ν

Object	Estimated Parameters			Parameters of Fit				
	f_G	α_{max}	E_{B-V}	f_G	f_R	α	E_{B-V}	σ
Mrk 176	0.70	1.6	0.04	0.70	0.00	1.0	0.04	0.03
3C 33	0.76	1.3	0.05	0.81	0.01	1.2	0.07	0.03
Mrk 3	0.73	0.7	0.11	0.78	0.05	0.7	0.18	0.05
NGC 1068	0.70	1.0	0.04	0.75	0.03	1.0	0.00	0.06
Mrk 573	0.93	0.5	0.04	0.88	0.02	0.2	0.03	0.02
Mrk 78	0.86	0.9	0.08	0.86	0.02	0.2	0.04	0.03
Mrk 348	0.91	0.8	0.08	0.86	0.01	0.6	0.08	0.04
Mrk 34	0.63	0.9	0.05	0.68	0.04	0.8	0.00	0.04
Mrk 1	0.72	0.9	0.08	0.77	0.03	0.8	0.13	0.06
3C 184.1	0.63	1.2	0.08	0.63	0.02	1.2	0.14	0.08
3C 433	0.68	1.7	0.14	0.80	0.01	1.6	0.33	0.02
Mrk 270	0.98	0.4	0.05	0.88	0.01	0.2	0.02	0.02
III Zw 55	0.52	1.9	0.06	0.60	0.01	1.8	0.15	0.02
3C 452	0.95	1.0	0.15	0.95	0.00	1.0	0.27	0.02
Mrk 198	0.65	1.5	0.03	0.65	0.01	1.5	0.05	0.03
Mrk 268	0.81	1.3	0.03	0.81	0.01	1.3	0.09	0.02
Mrk 273	0.33:	1.7	0.04	0.65	0.01	1.8	0.07	0.08
I Zw 81	0.75	2.0	0.04	0.75	0.00	0.8	0.04	0.02
Mrk 298	0.83	1.0	0.05	0.83	0.02	1.0	0.05	0.02
Mrk 507	0.68	1.4	0.08	0.73	0.01	1.4	0.18	0.03
Mrk 700	0.54	1.6	0.07	0.64	0.01	0.8	0.01	0.08
NGC 6764	0.43	1.4	0.14	0.33	0.02	0.2	0.18	0.04
Mrk 378	0.56:	1.9	0.10	0.56	0.01	1.5	0.10	0.04
Mrk 6	0.46	0.8	0.09	0.65	0.07	0.7	0.20	0.14
Mrk 315	0.26	1.4	0.07	0.45	0.02	1.3	0.23	0.02
Mrk 372	0.84	1.0	0.07	0.89	0.01	0.9	0.17	0.04
Mrk 42	0.15:	1.4	0.03	0.25	0.03	1.2	0.01	0.05
5C 3.100	0.29	1.9	0.11	0.29	0.01	1.8	0.09	0.05
3C 98	0.8	2.9	0.08	0.80	0.00	2.8	0.08	0.04
3C 178	0.8	2.2	0.95	0.80	0.01	2.0	0.30	0.03
3C 192	0.8	2.3	0.09	0.85	0.01	2.3	0.20	0.05
3C 327	0.8	2.0	0.06	0.80	0.01	2.0	0.16	0.02
PKS 2322-12	0.8	1.7	0.04	0.75	0.02	1.2	0.00	0.03

subtraction process is denoted f_G and was typically about 0.70.

If the Balmer emission lines result from recombination, there will be a recombination continuum due to H^+ (and also He^+ and He^{++}). Further, there will be two-photon decay of the $2\,^2S$ level of hydrogen. This continuum as given by Brown and Mathews (1970) accounts for about 2% of the continuum at λ4861 ($= f_R$).

The remaining approximately 30% of the continuum at λ4861 is basically what appears after subtracting the absorption-line spectrum. This featureless continuum may be a power law which, if extended to high energies, might photoionize the gas. If one postulates that there is a power law of the form $F_\nu \propto \nu^{-\alpha}$ and that the power law contains enough ultraviolet photons to photoionize H^0, He^0, and He^+ to produce by recombination the observed line fluxes of Hβ, He I λ5876, and He II λ4686, then there is a maximum power-law index, α_{max}, for which this is possible. Power laws with $\alpha < \alpha_{max}$ have more than enough ultraviolet photons to accomplish this. Typical values of α_{max} are about 1.3.

One cannot directly compare the power-law index of the remaining featureless continuum with α_{max}. An additional complication is the reddening of the stellar continuum by the extinction in our own Galaxy, and possibly in the other galaxy too. When comparing the observed continuum intensities of the emission-line galaxies with those of the galaxies without emission lines, differences in the amount of reddening may be attributed erroneously to differences in the amount of an underlying power-law continuum and to differences in its power-law index. The decomposition of the observed continuum is not unique. Rather more useful is to make a test for consistency.

In Table 8 as "Estimated Parameters" are given the measured amount of stellar continuum at λ4861, f_G, the power-law index α_{max} needed to give the observed strength of Hβ, and the expected amount of reddening due to our Galaxy, E_{B-V}, as determined from the cosecant law given by Burstein and McDonald (1975). The five narrow-line radio galaxies from Costero and Osterbrock (1977) are included with f_G estimated to be 0.8. The observed continua in these galaxies were reduced to intensity measures at 10 points in the spectrum from λ3500 to λ7300 (Koski 1976). These points were fitted to a model of a power law with index α, a recombination continuum of strength f_R at λ4861, and a stellar continuum (defined by the average of NGC 6482 and NGC 6702 or by NGC 2681) of strength f_G at λ4861 which is reddened by an amount of E_{B-V}. Satisfactory fits were those with $\alpha < \alpha_{max}$, f_G within 0.1 (the estimated error) of the estimated

value, and E_{B-V} within 0.13 (the standard error) of the estimated value from the cosecant law. Generally the fits were good, with the best ones listed in Table 8. The standard deviation of the fit σ is given in units of the observed continuum intensity at λ4861 and is typically about 0.04. The average amount of stellar continuum at λ4861 is 0.71 ± 0.17, and the average power-law index is 1.0 ± 0.5. The worst fit was for Mrk 6 which has a very strong continuum in the neighborhood of λ3727.

Overall the continua are consistent with a stellar background with an underlying power law which, if extrapolated to high energies, has enough ultraviolet photons to photoionize H^0 and to produce the observed strength of Hβ by recombination. The power law further contains enough high-energy photons to photoionize He^0 and He^+ to produce the observed strengths of He II λ4686 and He I λ5876 by recombination, except in two cases. The two galaxies Mrk 273 and III Zw 55 have He II λ4686 slightly too strong for the recombination value. If the observed power law is reddened, then there will be more ultraviolet photons which might be expected to give the stronger strengths of He II λ4686 in the above two objects.

The spectra with H absorption lines further distinguish themselves by having weak [O III] λ5007 compared to Hβ. If we exclude the three intermediate Seyfert galaxies and the three galaxies with extremely flat, blue continua (NGC 6764, Mrk 42, and 5C 3.100) and include the five radio galaxies reported by Costero and Osterbrock (1977) (one of which, 3C 178, has H absorption lines), then we have a sample of 21 galaxies without H absorption and six with H absorption. If we rank these galaxies by increasing strength of $I([O\ III]\ \lambda5007)/I(H\beta)$, then the ones with H absorption have ranks 2, 3, 5, 7, 9, and 10, with a sum equal to 36. The probability of the sum of the ranks being equal to or less than 36 on the basis of pure chance may be found by the Wilcoxon two-sample test (see, for instance, Hodges and Lehmann 1964, p. 303), and $P(W \leq 36) = 0.0017$. The presence of H absorption lines appears to signal the presence of a weaker source of ionization. The continuous spectrum which underlies the H absorption-line spectrum (which indicates early-type stars) may well be due to very hot OB stars rather than a power law. Indeed, a blackbody spectrum of 50,000 K provides enough ultraviolet photons to photoionize H and He and to reasonably account for the continuum which dilutes the galaxy spectrum in the optical region.

V. IONIZING SOURCE

All the galaxies presented here have emission lines in their spectra. All show an ultraviolet excess in their continua when compared with galaxies with no emission lines. From the strength of the stellar absorption features, all the galaxies have an underlying continuous spectrum. These observations suggest that the emission lines and continuous spectra are related phenomena. As shown in § IV, the continua are consistent with there being a component due to a power law which could photoionize enough H^0 to produce the observed strength of Hβ by recombination. Photoionization is suggested as the mechanism of energy input to the gas in these galaxies. This idea has been stated many times in the literature—for example, Greenstein and Schmidt (1964), Oke (1965), Osterbrock and Parker (1965, 1966), Searle and Sargent (1968), etc.

In § IV it was seen that the galaxies with Balmer absorption lines in their spectra (Mrk 198, Mrk 268, I Zw 81, Mrk 507, Mrk 700, and NGC 6764; and 3C 178 from Costero and Osterbrock 1977) have weak [O III] λ5007 emission. If one compares other line strengths in these galaxies (see Table 2) with those of normal galaxies with emission lines (see the spectra of M51 and M81 in Table 9), one sees that these weak-lined Seyfert galaxies are very much like normal galaxies. The values for M51 and M81 are ranges of observations of Peimbert (1968) and Warner (1973) for the smallest apertures given (7″ by Peimbert and 2″.5 by Warner). The observed line intensities have been corrected for a small amount of reddening by the authors. The emission relative to the continuum in the Seyfert galaxies is stronger than in these normal galaxies: Mrk 378 has an equivalent width of Hα, $W(H\alpha) = 27$ Å, and I Zw 81 has $W(H\alpha) = 16$ Å, whereas M51 and M81 have $W(H\alpha) = 14.6$ Å and 9.9 Å, respectively (using values from Peimbert 1968). In addition, the emission-line widths for Mrk 378 and I Zw 81 are 300 and 225 km s^{-1}, respectively, the two narrowest of the sample presented here. The galaxies Mrk 378 and I Zw 81 are probably not Seyfert galaxies (indeed, there was no suggestion of emission lines in Mrk 378 by Markarian and Lipovetsky 1971). They are transition cases between normal galaxies with emission lines and Seyfert 2 galaxies. All these galaxies with weak high-ionization emission lines appear to have sources of ionization similar to that in normal galaxies with emission lines.

The other Seyfert galaxies with stronger high-ionization emission lines have spectra very similar to one another. An average spectrum is given in Table 9 for these Seyfert 2 and narrow-line radio galaxies. The average spectrum is different from M51 and M81 because of the very strong [O III] λ5007 line in the Seyfert galaxies. It is also different from an H II region, the Orion Nebula, NGC 1976, from Johnson (1968) with 0.5 reddening correction applied. Not only are the high-ionization lines ([Ne V], [Ne III], [O III], He II, and [Fe VII]) stronger in the Seyfert spectrum, but the low-ionization lines ([O II], [N I], [O I], [N II], and [S II]) are also stronger. The harder radiation from the central star of a planetary nebula may be expected to give stronger high-ionization lines. Given in Table 9 are observations of the high-excitation planetary nebula NGC 7027 by Aller, Bowen, and Minkowski (1955) and Aller, Bowen, and Wilson (1963) which have been corrected for reddening. These values agree well with the intensities measured by O'Dell (1963). The agreement is now better, but the low-ionization lines remain stronger in the Seyfert spectrum. Finally we compare the spectrum with the Crab Nebula which

TABLE 9

RELATIVE LINE INTENSITIES CORRECTED FOR REDDENING

Line		M51 Nucleus	M81 Nucleus	Sy 2 NLRG	Orion Neb.	NGC 7027	Crab Neb.	MacAlpine Model 1	MacAlpine Model 2
3426	[Ne V]			1	...	1.3	0.3	0.3	0.8
3727	[O II]	1- 2	1-2	3	1.5	0.4	13	0.2	0.6
3869	[Ne III]			1.5	0.2	1	2	0.5	0.7
4071	[S II]			0.2	0.02	0.1			
4363	[O III]			0.2	0.02	0.3	0.2	0.2	0.5
4686	He II			0.3	...	0.5	0.7	0.2	0.3
4861	Hβ	1	1	1.0	1.0	1.0	1.0	1.0	1.0
5007	[O III]	2- 3	1	11	3.4	11	12	18	26
5199	[N I]			0.1	0.01	0.01			
5876	He I			0.1	0.28	0.1	0.8	0.06	0.06
6087	[Fe VII]			0.1	...	0.01		0.04	0.08
6300	[O I]	0.5	0.7	0.5	0.06	0.1	1.2	1.2	2.4
6583	[N II]	6-10	4-6	2.3	0.45	1	4	0.9	1.2
6724	[S II]	1- 2	1	1.5	0.11	0.05	9		
7136	[Ar III]			0.2	0.13	0.2			

is photoionized by a synchrotron continuum. The observations in Table 9 are a reddening-corrected average of a red and a green filament by Miller (1978). Now the low-ionization lines are much stronger than in a Seyfert galaxy (and the helium lines too because the He abundance is high). These lines are strong because the extremely high energy photons penetrate deeply into the neutral gas, freeing electrons by photoionization which can then collisionally excite the neutral atoms. A very good match to the average Seyfert galaxy spectrum is obtained by combining three-fourths the relative intensities of NGC 7027 with one-fourth those of the Crab Nebula. This suggests that a photon spectrum intermediate between that of a hot central star of a planetary nebula and a synchrotron continuum is needed to photoionize the gas in Seyfert 2 and narrow-line radio galaxies.

Seyfert photoionization models by MacAlpine (1971) are given in the last two columns of Table 9. Model 1 has the photoionizing photons coming from a power-law continuum with the spectral index = 1.2 and ionizing a gas of density 10^4 cm^{-3} with $N(\mathrm{He})/N(\mathrm{H}) = 0.06$ and a filling factor of 10^{-2}. Model 2 is similar, but the source of the ionizing photons is a 500 km s^{-1} shock wave which produces a free-free continuum and line emission. In both models the lines of N and Ne are too weak to agree with the average Seyfert 2 spectrum. Peimbert (1968) found an overabundance of N in the nuclei of M51 and M81, so perhaps an increase in the abundances of N and Ne in MacAlpine's models would remove this discrepancy. Lines of [O I] and [O III] are too strong in the model, but [O II] λ3727 is much too weak. Some of the weakness of [O II] in the calculated model is due to collisional de-excitation of the ^2D level at the assumed density of 10^4 cm^{-3}, which is much greater than the average density of 2000 cm^{-3} found in § III*c*. In addition, Shields and Oke (1975) in a model for NGC 1068 and Boksenberg and Netzer (1977) in a model for the narrow-line component of NGC 3516 found that the calculated strength of [S II] λλ6716, 6731 was much less than that observed (also true for [O II] λ3727 and [N II] λλ6548, 6583). Most of the galaxies presented here have line strengths of the low-ionization ions relative to Hβ greater than in NGC 1068. Thus the conclusions reached by these authors apply to all the Seyfert 2 and narrow-line radio galaxies: Lines from ions of low ionization cannot arise from photoionization solely by the nonthermal continuum. Diffuse radiation, radiation from hot stars, or a time-dependent model as suggested by Shields and Oke, or some other process must be responsible for the conditions in the region of low ionization. The conditions in the low-ionization region will not necessarily be correlated with the conditions in the high-ionization region.

VI. CONCLUSIONS

We have found that there are no distinguishing differences between the spectra of Seyfert 2 galaxies and narrow-line radio galaxies. The emission spectra are rich with lines from a wide range of levels of ionization. The continuum is stellar light diluted by an underlying continuous spectrum. The line widths of both classes of galaxies have the same distribution, with the average full width at half-maximum intensity about 500–600 km s^{-1}.

There are three transitional effects: two between these galaxies and Seyfert 1 galaxies, and one between these galaxies and normal galaxies. The intermediate Seyfert galaxies have continua and broad Balmer-line components as do Seyfert 1 galaxies, but the narrow Balmer-line components and forbidden lines have strengths and widths identical with the Seyfert 2 spectra. The two galaxies with the strong Fe II emission, Mrk 42 and 5C 3.100, have spectra very much like Seyfert 1 galaxies: strong blue continuum, strong Fe II, and weak forbidden lines. Only their line widths (permitted and forbidden lines have the same width) place them in the Seyfert 2 or narrow-line radio galaxy class. As for transitions to the normal galaxies with emission lines, a few galaxies have very weak high-ionization lines. The strength of the lines present

in their spectra are very much like those in normal galaxies. All in all, the Seyfert 2–narrow-line radio galaxy class is a fairly well defined class with fuzzy edges.

There appear to be two ionization regions in these galaxies: high and low ionization. The strength of emission lines from the two regions are separately correlated, and several emission-line objects show a redshift difference between lines arising in the two regions.

Photoionization as the energy input to the gas seems quite likely. All the galaxies show an ultraviolet excess in their spectra. Those galaxies with strong high-ionization emission lines have continua which are consistent with power-law continua extending to high energies.

The present classification system for Seyfert galaxies based on line widths is very good, but perhaps some of its limitations have been reached. As small changes, I suggest that the Seyfert 2 phenomenon refer only to those spectra with strong emission lines of high ionization ions like [O III], [Ne V], and He II. And Seyfert 1 phenomena should include those objects with flat blue continua, strong Fe II emission, and weak forbidden lines irrespective of the line widths.

I am most grateful to D. E. Osterbrock for providing the Lick scanner data for this study. I am especially thankful for his teaching, guidance, and encouragement. I am also indebted to M. M. Phillips, R. Costero, and S. A. Grandi for assistance in observing and data reduction, and to J. A. Baldwin and S. A. Hawley for help in programming. Many conversations with G. M. MacAlpine and F. R. Feldman are greatly appreciated. I am thankful for the partial support of this research from NSF grant AST 76-18440 to D. E. Osterbrock and for the present support of NASA grant NGR-23-005-464 to W. A. Hiltner.

REFERENCES

Adams, T. F. 1973, *Ap. J.*, **179**, 417.
Aller, L. H., Bowen, I. S., and Minkowski, R. 1955, *Ap. J.*, **122**, 62.
Aller, L. H., Bowen, I. S., and Wilson, O. C. 1963, *Ap. J.*, **138**, 1013.
Anderson, K. S. 1970, *Ap. J.*, **162**, 743.
Angel, J. R. P., Stockman, H. S., Woolf, N. J., Beaver, E. A., and Martin, P. G. 1976, *Ap. J.* (*Letters*), **206**, L5.
Boksenberg, A., and Netzer, H. 1977, *Ap. J.*, **212**, 37.
Brocklehurst, M. 1971, *M.N.R.A.S.*, **153**, 471.
Brown, R. L., and Mathews, W. G. 1970, *Ap. J.*, **160**, 939.
Burbidge, E. M. 1970, *Ap. J.* (*Letters*), **160**, L33.
Burbidge, E. M., and Strittmatter, P. A. 1972, *Ap. J.* (*Letters*), **172**, L37.
Burstein, D., and McDonald, L. H. 1975, *A.J.*, **80**, 17.
Costero, R., and Osterbrock, D. E. 1977, *Ap. J.*, **211**, 675.
Feldman, F. R. 1977, private communication.
Garstang, R. H. 1968, in *IAU Symposium No. 34, Planetary Nebulae*, ed. D. E. Osterbrock and C. R. O'Dell (Dordrecht: Reidel).
Grandi, S. A. 1977, *Ap. J.*, **215**, 446.
Greenstein, J. L., and Schmidt, M. 1964, *Ap. J.*, **140**, 1.
Hodges, J. L., and Lehmann, E. L. 1964, *Basic Concepts of Probability and Statistics* (San Francisco: Holden-Day).
Johnson, H. M. 1968, in *Nebulae and Interstellar Matter*, ed. B. M. Middlehurst and L. H. Aller (Chicago: University of Chicago Press), p. 65.
Khachikian, E. Ye., and Weedman, D. W. 1971, *Astrofizika*, **7**, 389.
———. 1974, *Ap. J.*, **192**, 581.
Koski, A. T. 1976, Ph.D. thesis, University of California, Santa Cruz.
Koski, A. T., and Osterbrock, D. E. 1976, *Ap. J.* (*Letters*), **203**, L49.
MacAlpine, G. M. 1971, Ph.D. thesis, University of Wisconsin.
Markarian, B. E., and Lipovetsky, V. A. 1971, *Astrofizika*, **7**, 511.
———. 1974, *Astrofizika*, **10**, 307.
Miller, J. S. 1968, *Ap. J.* (*Letters*), **154**, L57.
Miller, J. S. 1978, *Ap. J.*, **220**, 490.
Miller, J. S., and Mathews, W. G. 1972, *Ap. J.*, **172**, 593.
Miller, J. S., Robinson, L. B., and Wampler, E. J. 1976, *Advances in Electronics and Electron Physics* (New York: Academic Press), Vol. **40B**, p. 693.
O'Dell, C. R. 1963, *Ap. J.*, **138**, 1018.
Oke, J. B. 1965, *Ap. J.*, **141**, 6.
Osterbrock, D. E. 1974, *Astrophysics of Gaseous Nebulae* (San Francisco: Freeman).
———. 1976, *Pub. A.S.P.*, **88**, 589.
Osterbrock, D. E., and Koski, A. T. 1976, *M.N.R.A.S.*, **176**, 61P.
Osterbrock, D. E., Koski, A. T., and Phillips, M. M. 1975, *Ap. J.* (*Letters*), **197**, L41.
Osterbrock, D. E., and Miller, J. S. 1975, *Ap. J.*, **197**, 535.
Osterbrock, D. E., and Parker, R. A. R. 1965, *Ap. J.*, **141**, 892.
———. 1966, *Ap. J.*, **143**, 268.
Peimbert, M. 1968, *Ap. J.*, **154**, 33.
Phillips, M. M. 1976, *Ap. J.*, **208**, 37.
Robinson, L. B., and Wampler, E. J. 1972, *Pub. A.S.P.*, **84**, 161.
———. 1973, in *Astronomical Observations with Television-Type Sensors*, ed. J. W. Glaspey and G. A. H. Walker (Vancouver: University of British Columbia), p. 69.
Rubin, V. C., Thonnard, N., and Ford, W. K. 1975, *Ap. J.*, **199**, 31.
Sargent, W. L. W. 1970, *Ap. J.*, **160**, 405.
Schmidt, M. 1965, *Ap. J.*, **141**, 1.
Searle, L., and Sargent, W. L. W. 1968, *Ap. J.*, **153**, 1003.
Seaton, M. J. 1975, *M.N.R.A.S.*, **170**, 475.
Shectman, S. A., and Hiltner, W. A. 1976, *Pub. A.S.P.*, **88**, 960.
Shields, G. A., and Oke, J. B. 1975, *Ap. J.*, **197**, 5.
Wampler, E. J. 1968, *Ap. J.* (*Letters*), **154**, L53.
———. 1971, *Ap. J.*, **164**, 1.
Warner, J. W. 1973, *Ap. J.*, **186**, 21.
Weedman, D. W., and Khachikian, E. Ye. 1969, *Astrofizika*, **5**, 113 (English transl., p. 51).
Zwicky, F. 1971, *Catalogue of Selected Compact Galaxies and of Post-Eruptive Galaxies* (Guemligen: Zwicky), p. 224.

ALAN T. KOSKI: Department of Astronomy, University of Michigan, Ann Arbor, MI 48109